THE JOURNAL OF PHYSICAL CHEMISTRY A

Article

pubs.acs.org/JPCA

Rotational Mode Specificity in the F^- + CH_3Y [Y = F and Cl] S_N2 Reactions

István Szabó[†] and Gábor Czakó*[,†]

Laboratory of Molecular Structure and Dynamics, Institute of Chemistry, Eötvös University, P.O. Box 32, H-1518 Budapest 112, Hungary

ABSTRACT: More than 12 million quasiclassical trajectories are computed for the F^- + $CH_3Y(v = 0, JK)$ [Y = F and Cl] S_N2 reactions using full-dimensional ab initio analytical potential energy surfaces. The initial (J, K = 0) and (J, $K = J$) [J = 0, 2, 4, 6, 8] rotational state specific cross sections are obtained at different collision energies (E_{coll}) in the 1−20 kcal mol^{-1} range, and the scattering angle and initial attack angle distributions as well as the mechanism-specific opacity functions are reported at E_{coll} = 10 kcal mol^{-1}. The tumbling rotation (K = 0) inhibits the F^- + CH_3F reaction by a factor of 3 for J = 8 at E_{coll} = 10 kcal mol^{-1}. This tumbling rotational effect becomes smaller at low and high E_{coll}, and the tumbling motion affects the cross sections of F^- + CH_3Cl by only a few percent. The spinning rotation ($K = J$) hinders both reactions by factors in the 1.3−1.7 range for J = 8 at low E_{coll}, whereas slight promotion is found as the E_{coll} increases. The tumbling rotation may counteract the attractive ion-dipole forces, and the spinning motion hinders the complex formation, thereby decreasing the reactivity.

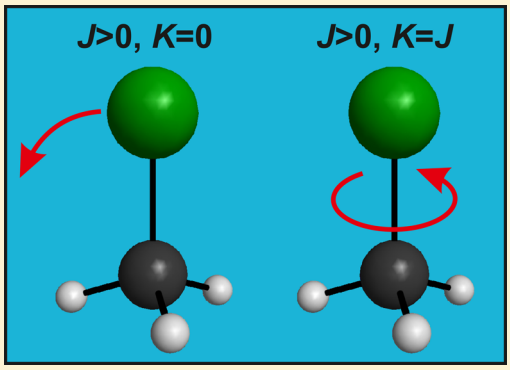

I. INTRODUCTION

Chemical reactivity depends on how the total energy of the systems is distributed among the translational, vibrational, and rotational degrees of freedom. For atom + diatom reactions both reactant's vibration and rotation can be characterized by single quantum numbers, v and J, respectively. Vibrational excitations usually promote the atom + diatom reactions, whereas the J dependence of the reactivity can be more complicated showing promotion or inhibition depending on the magnitude of J and the type of the system.[1−3] For polyatomic reactants the picture is even more complex. An N-atomic nonlinear molecule has $3N - 6$ vibrational modes, and the excitation of different modes can have different effects on the reactivity. Furthermore, symmetric or asymmetric polyatomic rotors are characterized by the total rotational angular momentum quantum number J and its projections, K (symmetric top) or K_aK_c (asymmetric top), to the body-fixed axes. The vibrational mode specificity in polyatomic reactions has been widely studied;[4−9] however, little is known about rotational mode specific, that is, K-dependent, effects on chemical reactivity. Nevertheless, there are a couple of recent experimental and theoretical studies on rotational mode specificity.[10−14] In 2012 rotational enhancement effects were observed experimentally for the $H_2O^+(J, K_a, K_c)$ + D_2 reaction,[10] and later in 2014, ab initio computations showed that rotational excitation facilitates the reorientation of H_2O^+, thereby enhancing the reactivity.[11] The JK-dependent reactivity of CHD_3 with H, Cl, and $O(^3P)$ was studied in 2014.[12−14] For H + $CHD_3(v = 0)$ → H_2 + CD_3 a seven-dimensional time-dependent wave packet study found that rotational excitation up to J = 2 has negligible effect on the reactivity.[12] For the Cl + $CHD_3(v_1 = 1)$ → HCl + CD_3 reaction a joint crossed-beam, quantum dynamics, and quasiclassical trajectory (QCT) study showed that tumbling rotation (K = 0) significantly increases the reactivity, whereas the spinning rotation ($K = J$) about the CH axis gives smaller enhancement factors.[13] Similar behavior was recently found by QCT calculations for the $O(^3P)$ + $CHD_3(v_1 = 0,1)$ → OH + CD_3 reactions.[14] In 2015 Liu and co-workers showed that the total reactivity (integral cross sections) of the Cl + $CHD_3(v_1 = 1)$ reaction depends on the initial JK states, but rotational excitations have virtually no effect on the angular distributions (differential cross sections).[15] A previous QCT study reported the same findings for the $O(^3P)$ + CHD_3 reaction.[14] In 2015 the rotational effects in the OH + CH_3 → O + CH_4 reaction were studied by Wang and co-workers using six- and seven-dimensional quantum models.[16,17] It was shown, albeit not JK specifically, that the rotational excitation of CH_3 (and OH) significantly hinders the reactivity.

The polyatomic reactant in the X^- + CH_3Y [X,Y = F, Cl, Br, I] bimolecular nucleophilic substitution (S_N2) reactions is a symmetric top, like the above-discussed CHD_3 molecule. Although the dynamics of S_N2 reactions have been widely studied,[18−23] to the best of our knowledge, the JK rotational state specific reactivity of S_N2 reactions has not been investigated yet. We recently developed global full-dimensional

Special Issue: Dynamics of Molecular Collisions XXV: Fifty Years of Chemical Reaction Dynamics

Received: June 29, 2015
Revised: July 27, 2015
Published: August 10, 2015

DOI: 10.1021/acs.jpca.5b06212
J. Phys. Chem. A 2015, 119, 12231−12237

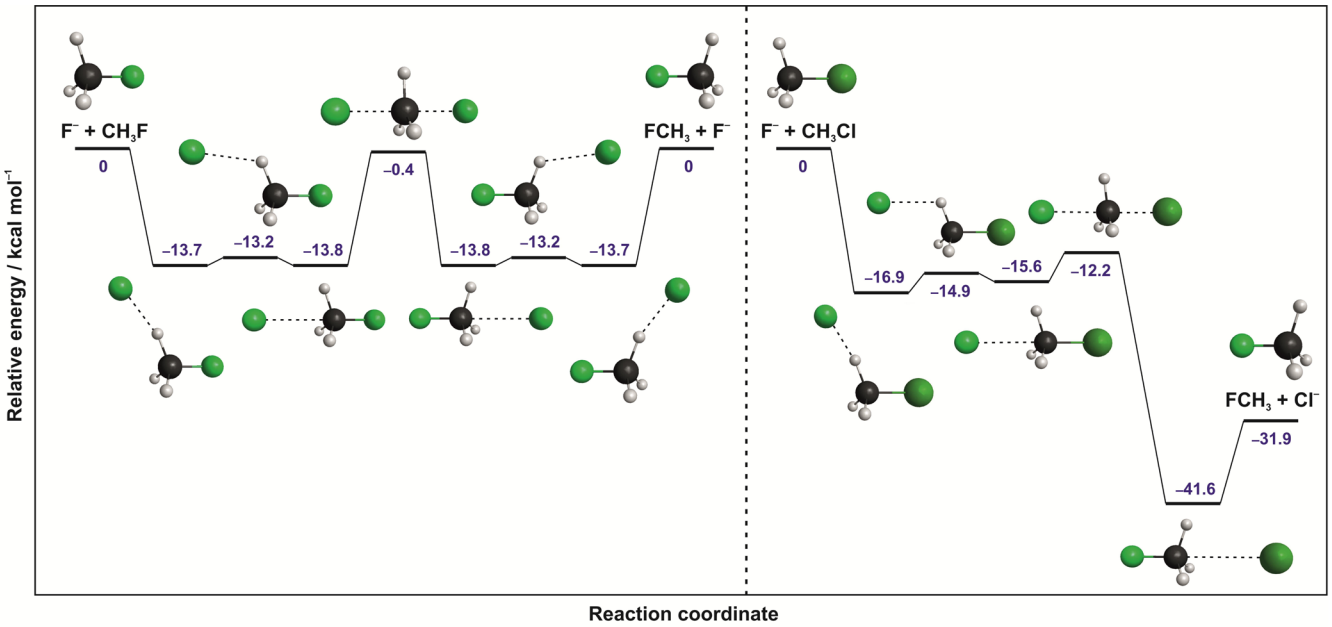

Figure 1. Schematic energy diagram of the $F^- + CH_3F$ and $F^- + CH_3Cl$ reactions showing the stationary points of the S_N2 backside attack pathways. The accurate benchmark relativistic all-electron CCSDT(Q)/complete-basis-set quality focal-point energies, taken from refs 24 and 25, are relative to the $F^- + CH_3F(eq)$ and $F^- + CH_3Cl(eq)$ asymptotes.

analytical potential energy surfaces (PESs) for the $F^- + CH_3F$ (ref 24) and $F^- + CH_3Cl$ (ref 25) reactions by fitting high-level coupled-cluster-based ab initio energy points. In the present study we investigate the *JK*-dependence of the reactivity of the $F^- + CH_3Y(v = 0, JK)$ [Y = F and Cl] S_N2 reactions by performing QCT calculations on the analytical PESs. Although both CHD_3 and CH_3Y are symmetric tops, CHD_3 is an oblate-type rotor with rotational constants $A = B = 3.29$ and $C = 2.64$ cm^{-1}, whereas CH_3Y is a prolate top with $A = 5.25/5.27$ and $B = C = 0.86/0.44$ cm^{-1} for Y = F/Cl. The $X + CHD_3$ [X = H, Cl, $O(^3P)$] reactions are endothermic with substantial barriers,[9] whereas the S_N2 reactions $F^- + CH_3F$ and $F^- + CH_3Cl$ are isoenergetic with a slightly negative barrier and highly exothermic with negative barrier, respectively, as seen in Figure 1.[24,25] Furthermore, in the S_N2 reactions one can expect significant stereodynamical effects due to the relatively strong long-range attractive ion-dipole forces, whereas in the $X + CHD_3$ reactions only weak van der Waals interactions can occur. Thus, the very different rotational constants and PES shapes indicate that the state-specific rotational excitations may have different effects on the dynamics of the $X + CHD_3$ and $F^- + CH_3Y$ reactions. In Section II we describe the quasiclassical initial *JK*-specific rotational mode sampling and give the details of the QCT calculations. In Section III we present the *JK*-dependent QCT results for the $F^- + CH_3Y(v = 0, JK)$ S_N2 reactions and compare the rotational effects for two different leaving groups, Y = F and Cl. The paper ends with summary and conclusions in Section IV.

II. METHODS

QCT computations are performed for the $F^- + CH_3F$ and $F^- + CH_3Cl$ reactions using the recently developed full-dimensional analytical ab initio PESs.[24,25] According to the standard QCT methodology,[26] the vibrational energy of the polyatomic reactants is set to the zero-point energy (ZPE) by random distribution of the harmonic ground state ($v = 0$) mode-specific vibrational energy in the phase space of each normal mode. The initial rotational quantum numbers (*JK*) for the CH_3F and CH_3Cl reactants are set following the procedure described in detail below.

A. Rotational Mode Sampling. If the rigid-rotor approximation is assumed, the CH_3F and CH_3Cl molecules are prolate-type symmetric tops characterized by the *J* and *K* rotational quantum numbers. The length of the classical angular momentum vector (**j**) is related to the *J* quantum number according to (in atomic units)

$$j = \sqrt{J(J+1)} \tag{1}$$

where *j* satisfies the following relation:

$$j = \sqrt{j_x^{\,2} + j_y^{\,2} + j_z^{\,2}} \tag{2}$$

In principal axis system (PAS) the j_x^{PAS} component of the angular momentum vector corresponds to the *K* projection quantum number:

$$j_x^{PAS} = K \tag{3}$$

(Note that this convention applies only to prolate-type symmetric tops.) To perform computations with fixed *J* and *K*, the two remaining components of **j** should be sampled employing the following expressions:

$$j_y^{PAS} = (j^2 - K^2)^{1/2} \sin 2\pi R \tag{4}$$

$$j_z^{PAS} = (j^2 - K^2)^{1/2} \cos 2\pi R \tag{5}$$

where $R \in [0, 1]$ is a real random number. Note that eqs 3, 4, and 5 satisfy eq 2. The $\mathbf{j}^{PAS}$ vector is then transformed to the space-fixed Cartesian coordinate system, defined during the QCT computation, using the similarity transformation matrix obtained by the diagonalization of the moment of inertia tensor (**I**). The desired angular momentum **j** is tuned[26] by the modification of the velocity vectors for each atom

DOI: 10.1021/acs.jpca.5b06212
J. Phys. Chem. A 2015, 119, 12231−12237

$$\mathbf{v}_i = \mathbf{v}_i^0 + \mathbf{\Omega} \times \mathbf{q}_i \quad (6)$$

where $\mathbf{\Omega} = \mathbf{I}^{-1}(\mathbf{j} - \mathbf{j}_0)$, and $\mathbf{q}_i$ stands for the Cartesian coordinates of the ith atom, and $\mathbf{j}_0$ denotes the preexisting angular momentum.

B. Computational Details. The initial orientation of CH_3Y is randomly selected and the distance of its center of mass from F^- is $(x^2 + b^2)^{1/2}$, where b is the impact parameter scanned with a step size of Δb from 0 to b_{max}, where b_{max} is the maximum value of b, where reactive substitution event can occur. The settings for x, Δb, and b_{max} values at each collision energy (E_{coll}) are shown in Table 1. Trajectories are run at E_{coll} = 1, 2, 4, 7, 10, 15, and 20 kcal mol^{-1} and J values are increased from 0 to 8 with ΔJ = 2 and K = 0 or J. At each b, 5000 trajectories are computed, resulting in a total number of ∼12.5 million trajectories in this study. The trajectories are propagated using a 0.0726 fs time step, and each trajectory is stopped when the maximum of the actual interatomic distances is 1 bohr larger than the initial one. The ZPE constraint decreases the absolute cross sections, as it was shown previously for the substitution channel of the F^- + CH_3F reaction,[24] but does not have significant effects on the cross-section ratios and angular distributions. For the highly exothermic F^- + CH_3Cl S_N2 reaction the product ZPE violation is even less significant; therefore, we consider only the nonconstrained results.

Table 1. Settings for the Initial Distance of the Reactants and Impact Parameter Scans (in bohr) and the Total Number of Trajectories at Each Collision Energy (in kcal mol^{-1}) and Each JK Rotational State[a]

E_{coll}	x	Δb	b_{max}	N_{traj}
		F^- + $CH_3F(v = 0, JK)$		
1	25	1.0	23	120 000
2	20	1.0	15	80 000
4	20	0.5	10	105 000
7	20	0.5	8	85 000
10	20	0.5	7	75 000
15	20	0.5	7	75 000
20	20	0.5	6	65 000
		F^- + $CH_3Cl(v = 0, JK)$		
1	30	1.0	28	145 000
2	25	1.0	21	110 000
4	20	1.0	19	100 000
7	20	1.0	16	85 000
10	20	0.5	12	125 000
15	20	0.5	10	105 000
20	20	0.5	9	95 000

[a]The initial distance of the reactants is $(x^2 + b^2)^{1/2}$, where b = 0, Δb, 2Δb, ..., b_{max} and $N_{traj} = (b_{max}/\Delta b + 1) \times 5000$.

III. RESULTS AND DISCUSSION

The JK initial rotational state specific integral cross sections and the rotational enhancement factors for the F^- + $CH_3Y(v = 0, JK)$ [Y = F and Cl] S_N2 reactions in the 1−20 kcal mol^{-1} E_{coll} range are shown in Figure 2. The excitation function (cross sections vs E_{coll}) of the F^- + CH_3Cl reaction decreases rapidly with increasing E_{coll}, as expected for an exothermic barrierless reaction. The cross sections of the F^- + CH_3F reaction are approximately an order of magnitude smaller and decrease at low E_{coll}, have a minimum at E_{coll} ≈ 4−7 kcal mol^{-1} and become nearly constant above E_{coll} = 10 kcal mol^{-1}. In the present study the cross sections are investigated in the 1−20 kcal mol^{-1} E_{coll} range, but as shown in ref 24 the J = 0 excitation function of F^- + CH_3F remains almost constant up to E_{coll} = 80 kcal mol^{-1}. The shape of the J > 0 excitation functions at E_{coll} larger than 20 kcal mol^{-1} may be different. Furthermore, we should note that at low E_{coll} the ZPE violation effect on the absolute cross sections is significant for F^- + CH_3F, as discussed in ref 24.

The $(JK)/(J = 0)$ cross-section ratios show that rotational excitations usually inhibit the reactivity in the 1−20 kcal mol^{-1} E_{coll} range for both the F^- + CH_3F and F^- + CH_3Cl reactions. As Figure 2 shows, the inhibition factors depend sensitively on the J and K rotational quantum numbers, E_{coll}, and the leaving group. For F^- + CH_3F, the K = 0 rotational effects are small (∼10%) at low and high E_{coll} values, whereas the inhibition is substantial around E_{coll} = 10 kcal mol^{-1}. At E_{coll} = 10 kcal mol^{-1} the K = 0 rotational enhancement factors are 0.93, 0.74, 0.56, and 0.35 for J = 2, 4, 6, and 8, respectively. For the $K = J$ states the rotational enhancement factors are in the 0.6−1.0 range for E_{coll}'s up to ∼10 kcal mol^{-1} and tend to 1.0−1.1 as E_{coll} increases. The picture is quite different for the F^- + CH_3Cl reaction. For the $CH_3Cl(J, K = 0)$ states the rotational effects are negligible, as the enhancement factors are ∼0.95−1.0 for J up to 8. If $K = J$, the rotational effects are larger, for example, the enhancement factors are in the 0.9−1.0 range for J = 4 and in the 0.75−0.9 range for J = 8. These $CH_3Cl(J, K = J)$ enhancement factors are the most significant at low E_{coll}, especially at E_{coll} = 10 kcal mol^{-1}, and increase in the E_{coll} range of 10−20 kcal mol^{-1}. At E_{coll} = 10 kcal mol^{-1}, the enhancement factors are 0.97, 0.89, 0.79, and 0.75 for J = 2, 4, 6, and 8, respectively, whereas the corresponding values at E_{coll} = 20 kcal mol^{-1} are 1.03, 1.00, 0.94, and 0.90. As seen, at E_{coll} = 20 kcal mol^{-1} the (JK) = (22) state starts to promote the reaction, and we expect promotion for higher J values as well, as we further increase E_{coll}. To check this, we have computed the (JK) = (44) enhancement factor at E_{coll} = 30 kcal mol^{-1}, which turned out 1.06.

Before we move forward, let us consider the "rotational modes" of the CH_3Y molecule. The $(J > 0, K = 0)$ case means that the classical angular momentum vector is perpendicular to the CY axis (C_3 axis); thus, this motion corresponds to tumbling rotation. For $(J > 0, K = J)$, the angular momentum vector is parallel with the CY axis, resulting in spinning rotation about the CY bond. Since CH_3Y is a prolate top, where $A \gg B = C$, the angular velocity of the spinning rotation is significantly larger than that of the tumbling rotation.

To get deeper insight into the mechanistic origin of the rotational effects we computed the product angular and initial attack angle distributions as well as the opacity functions (reaction probabilities vs b) at E_{coll} = 10 kcal mol^{-1}, as shown in Figures 3 and 4, respectively. (E_{coll} = 10 kcal mol^{-1} is chosen, because the rotational effects are the most significant at this E_{coll}.) The attack angle (α) is defined at the beginning of each trajectory as the angle between the velocity vector of CH_3Y and the CY vector. Thus, α = 0° corresponds to frontal attack, and α = 180° means backside attack initial orientation. On the basis of the integration time, we could distinguish between direct and indirect trajectories as shown for the opacity functions in Figure 4.

For F^- + CH_3F, the J = 0 angular distributions show the dominance of backward scattering, which indicates the preference of the direct rebound mechanism at E_{coll} = 10 kcal mol^{-1} as shown in Figure 4. As we increase J while K = 0, the

DOI: 10.1021/acs.jpca.5b06212
J. Phys. Chem. A 2015, 119, 12231−12237

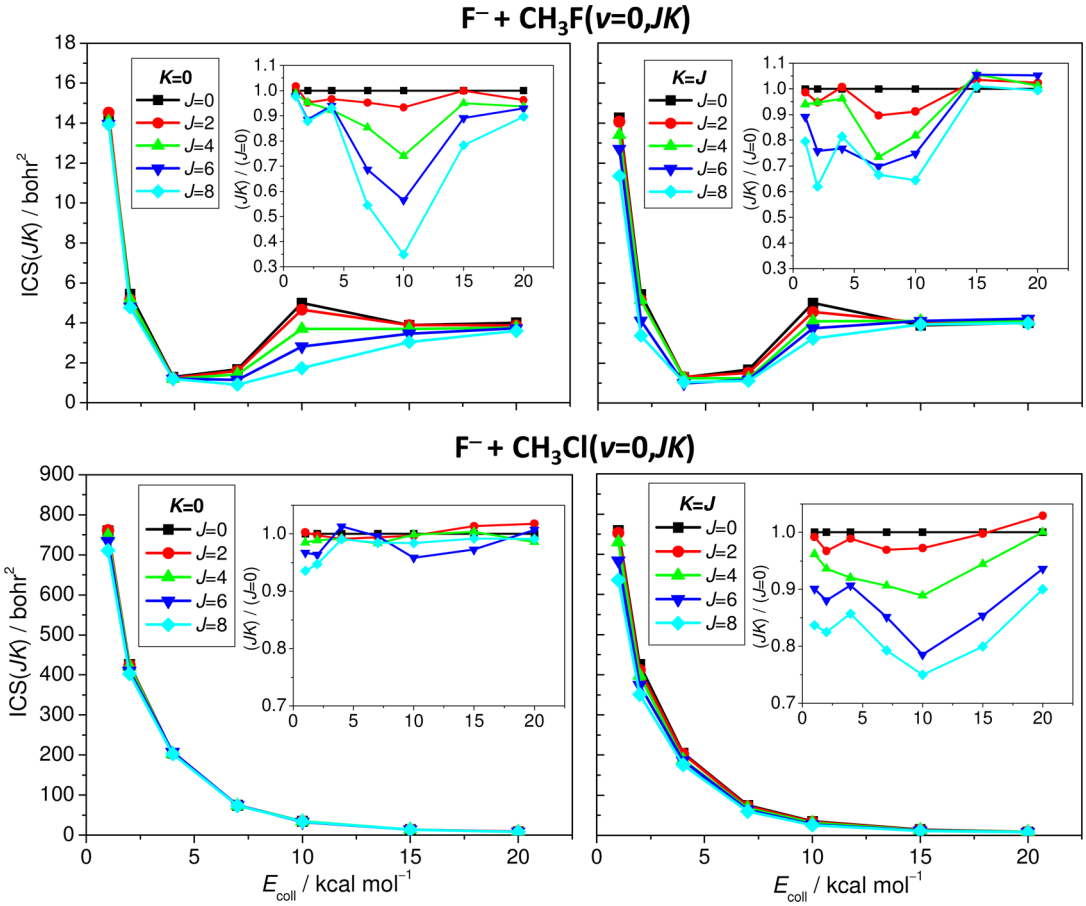

Figure 2. *JK*-dependence of the integral cross sections, ICS(*JK*), and their ratios, ICS(*JK*)/ICS(J = 0), for the F^- + CH_3F(v = 0, *JK*) → F^- + CH_3F and F^- + CH_3Cl(v = 0, *JK*) → Cl^- + CH_3F reactions as a function of collision energy.

angular distributions become more isotropic (Figure 3), which indicates that the indirect mechanisms dominate at high J. This is confirmed by the direct vs indirect (J = 8, K = 0) reaction probabilities shown in Figure 4. If $K = J$, the shift from direct to indirect mechanism is less significant; thus, the angular distributions show less pronounced J dependence. The J = 0 attack angle distributions show the preference of backside attack, whereas the (J > 0, K = 0) distributions show that the rotational excitation hinders the backside attack reactivity, while virtually not affecting the frontal attack reactivity. This suggests that the tumbling rotation counteracts the orientation effects, thereby decreasing the reactivity of the F^- + CH_3F reaction by a factor of 3 at E_{coll} = 10 kcal mol^{-1}. At lower and higher E_{coll} the K = 0 rotational effects are smaller (Figure 2). This may be because at low E_{coll} the reaction is mainly indirect even at J = 0 and at high E_{coll} the reaction is so direct and fast that the slow tumbling rotation cannot divert the trajectories from their reaction path. In the $K = J$ case, the spinning rotation does not significantly affect the attack angle distributions. However, at low E_{coll} in the 1−4 kcal mol^{-1} range, the rotational effects are found to be larger for $K = J$ than for K = 0. This may be explained by the fact that the relatively fast spinning rotation can inhibit the indirect substitutions by hindering the complex formations, which is not significantly affected by the slow tumbling motion.

In the case of the F^- + CH_3Cl reaction the rotational effects are less significant than those for F^- + CH_3F. For K = 0, the rotational inhibition is almost negligible, and the scattering angle and attack angle distributions are virtually not affected by rotational excitations. The J = 0 and (J = 8, K = 0) direct and indirect mechanism-specific opacity functions are also very similar. This shows that the tumbling rotation does not have any significant effect on the dynamics of the F^- + CH_3Cl reaction, whereas substantial inhibition was found for the F^- + CH_3F reaction at E_{coll} = 10 kcal mol^{-1}. This may be explained by the fact that the attractive forces are stronger in F^- + CH_3Cl than in F^- + CH_3F; thus, the tumbling rotation cannot counteract the steering effects for the former system. The potential profile shown in Figure 1 supports this statement, since the entrance-channel well is ∼2−3 kcal mol^{-1} deeper for F^- + CH_3Cl. The $K = J$ rotational excitations inhibit the F^- + CH_3Cl reaction and the effects are similar to those in F^- + CH_3F, as shown in Figure 2. The opacity functions reveal that the F^- + CH_3Cl reaction becomes more direct upon the excitation of the spinning rotation. Thus, the spinning rotational motion hinders the indirect reaction paths and makes most of the indirect trajectories nonreactive or speeds up their reactivity at small impact parameters.

One may wonder whether the different tumbling rotational effects found for the two reactions at E_{coll} = 10 kcal mol^{-1} originates from the different PESs or from the different rotational constants of the reactants. Rotational constant A is almost the same for CH_3F and CH_3Cl, whereas B is 0.86 and 0.44 cm^{-1} for CH_3F and CH_3Cl, respectively. This means that the spinning motion of CH_3F and CH_3Cl has similar angular velocity, whereas the tumbling rotation of CH_3F is about twice as fast as that of CH_3Cl. Does this explain the rotational effects? To address this question we performed QCT computations for

DOI: 10.1021/acs.jpca.5b06212
J. Phys. Chem. A 2015, 119, 12231−12237

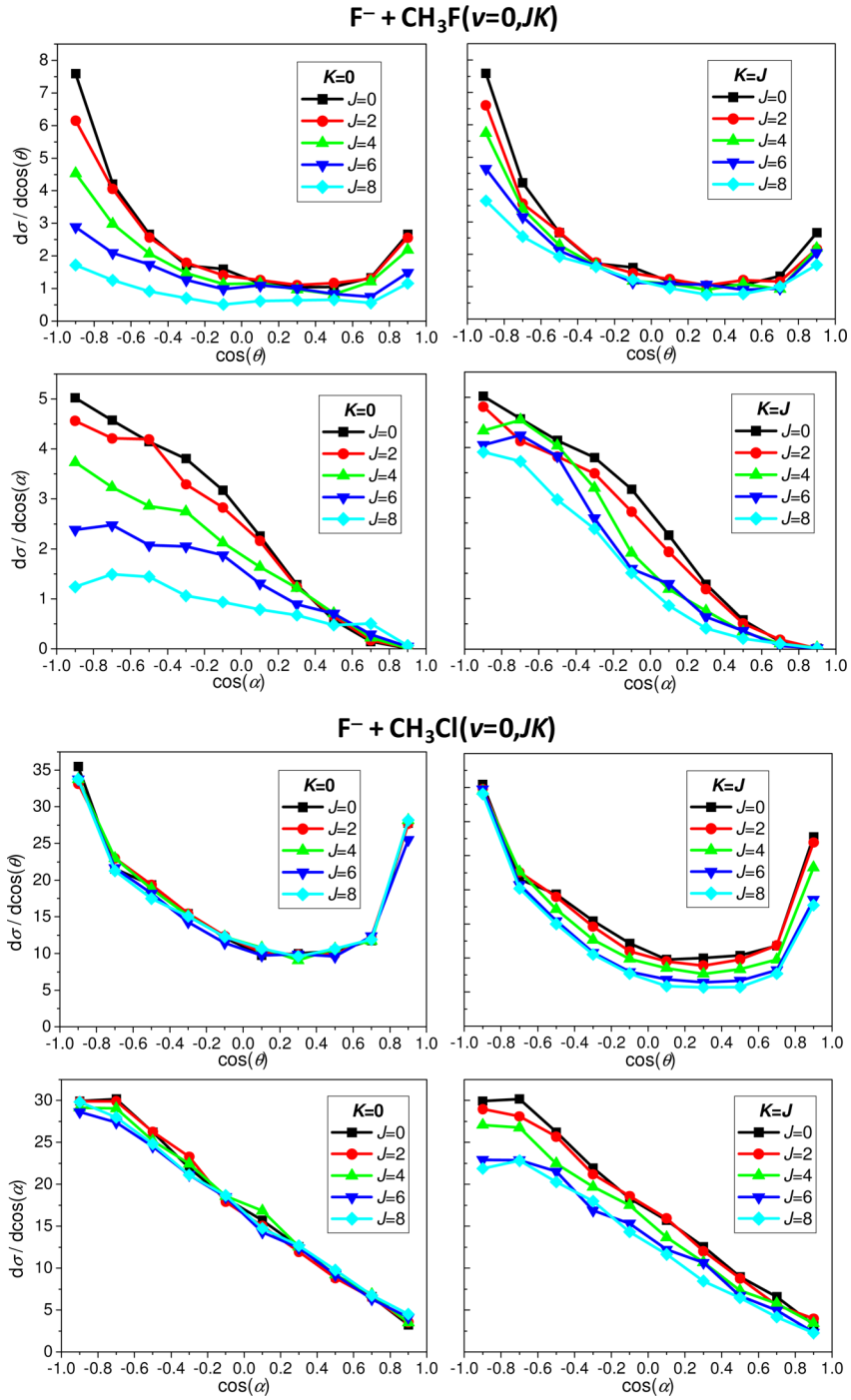

Figure 3. *JK*-dependence of the scattering angle (θ) and initial attack angle (α) distributions at collision energy of 10 kcal mol^{-1} for the $F^- + CH_3F(v = 0,JK) \rightarrow F^- + CH_3F$ and $F^- + CH_3Cl(v = 0,JK) \rightarrow Cl^- + CH_3F$ reactions.

the $F^- + CH_3F'$ reaction using the PES of $F^- + CH_3F$ and setting the mass of F′ to 35.5 amu. The opacity functions of the $F^- + CH_3F'$ reaction at E_{coll} = 10 kcal mol^{-1} are shown in Figure 4. As seen, the overall reaction probability decreases as we increased the mass of the leaving group; however, the mechanism-specific opacity functions are rather like $F^- + CH_3F$ than $F^- + CH_3Cl$. For $F^- + CH_3F'$ the $(J = 8)/(J = 0)$ cross-section ratios are 0.34(K = 0) and 0.71(K = J), which are very similar to the corresponding values of 0.35(K = 0) and 0.64(K = J) for $F^- + CH_3F$. Thus, we can conclude that the different tumbling rotational effects found for the two reactions are caused by the different PESs and not by the different rotational speed of the two reactants.

Finally, it is interesting to contrast the rotational mode specificity in the $F^- + CH_3Y$ [Y = F and Cl] S_N2 and the X + CHD_3 [X = Cl and O(^{3}P)] abstraction reactions. Unlike for the above-discussed S_N2 reactions, for X + CHD_3 rotational excitations enhance the reactivity and tumbling rotation has usually larger effects than spinning rotation.[13−15] This may be explained by considering the following facts: (a) unlike CH_3Y, CHD_3 is an oblate-type rotor, which means that the tumbling rotation of CHD_3 is faster than the spinning about the CH axis and (b) strong attractive forces present in the entrance channel

DOI: 10.1021/acs.jpca.5b06212
J. Phys. Chem. A 2015, 119, 12231−12237

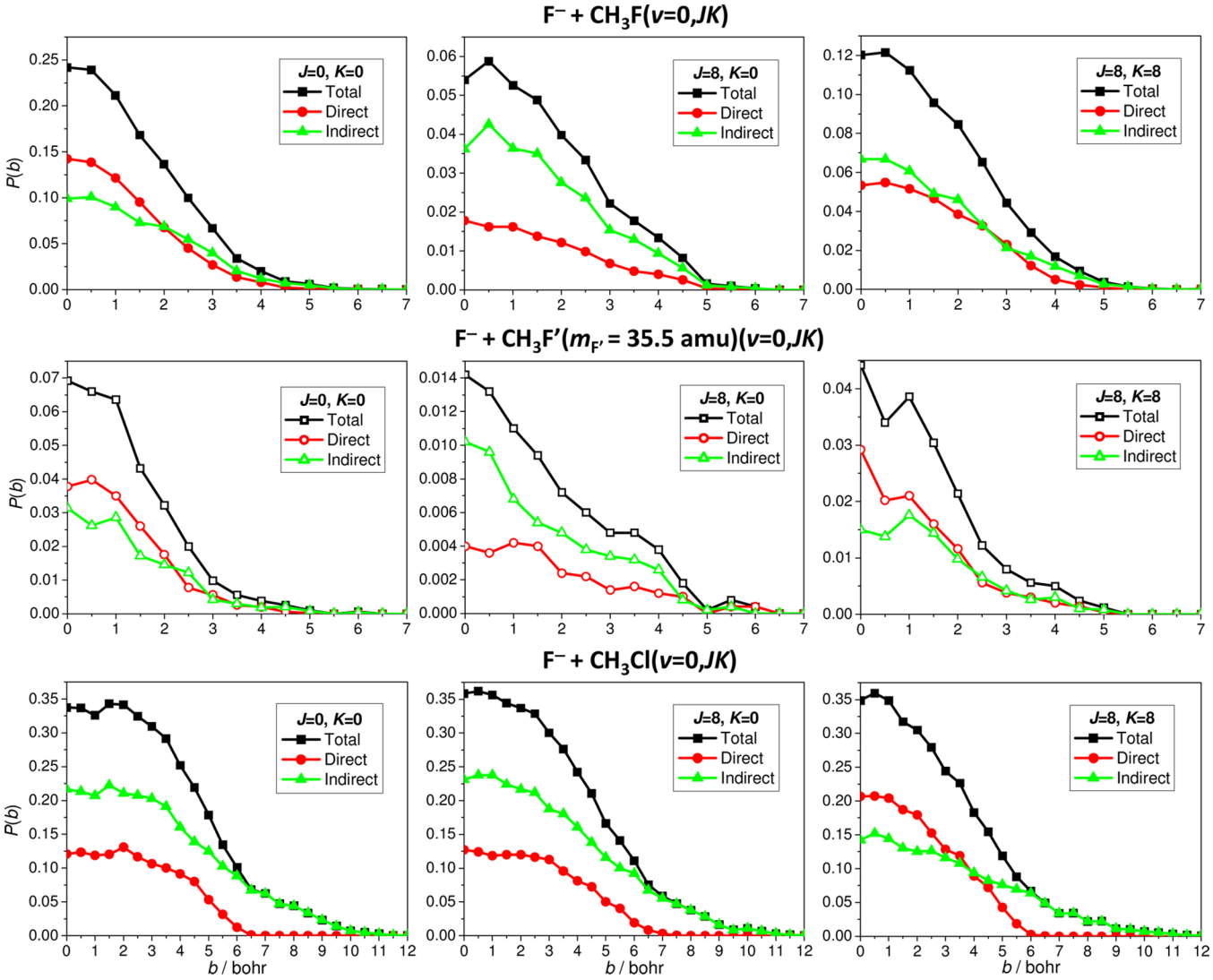

Figure 4. *JK*-dependence of the opacity functions at a collision energy of 10 kcal mol^{-1} for the $F^- + CH_3F(v = 0, JK) \rightarrow F^- + CH_3F$, $F^- + CH_3F'(v = 0, JK) \rightarrow F'^- + CH_3F$ ($m_{F'}$ = 35.5 amu), and $F^- + CH_3Cl(v = 0, JK) \rightarrow Cl^- + CH_3F$ reactions; the direct reaction probabilities were obtained from fast trajectories characterized by integration times lower than 0.65, 1.16, and 0.87 ps, respectively.

of the S_N2 reactions and the prereaction well is ∼13−17 kcal mol^{-1} deep involving H-bonded and ion-dipole complexes separated by barriers (Figure 1), whereas the van der Waals interactions for X + CHD_3 are weak resulting in a well depth of only ∼0.3−0.6 kcal mol^{-1}.[9] Thus, we may expect that that rotational motion counteracts the orientation effects in the S_N2 reactions, thereby inhibiting the reactions. In X + CHD_3 these steering effects are less pronounced; here the rotational motion, especially if $K = 0$, enlarges the range of the reactive attack angles, thereby promoting the reaction.[13−15] An alternative explanation of the different rotational effects may be related to the fact that the rotational energy can easily flow to the other degrees of freedom once the trajectory enters the deep well of the S_N2 reactions, whereas the X + CHD_3 reactions are much more direct without significant energy redistribution in the entrance channel.

IV. SUMMARY AND CONCLUSIONS

Following the pioneering initial rotational state specific studies on the reactions of the symmetric top CHD_3 molecule with Cl and O(^{3}P) atoms,[13−15] we have investigated the rotational mode specificity in the F^- + CH_3F and F^- + CH_3Cl S_N2 reactions. The QCT calculations utilized our recent full-dimensional ab initio analytical PESs[24,25] allowing the computation of ∼12.5 million trajectories, which is unprecedented for S_N2 reactions. The initial *JK*-specific cross sections show that the tumbling rotation ($K = 0$) inhibits significantly the F^- + CH_3F reaction at $E_{coll} \approx 10$ kcal mol^{-1}, whereas the tumbling rotational effects are almost negligible for the F^- + CH_3Cl reaction. The spinning rotation ($K = J$) hinders both S_N2 reactions at low E_{coll} and the inhibition diminishes and even slight promotion is seen as E_{coll} increases. For F^- + CH_3F the $K = 0$ rotational excitations made the scattering angle distributions more isotropic at E_{coll} = 10 kcal mol^{-1}, which correlates with the dominance of the indirect mechanisms characterized by the integration time. Test computations for the artificial F^- + CH_3F' reaction, where the mass of F′ is set to the mass of Cl, showed that the different PES shapes are responsible for the different rotational effects, because the change of the rotational constants of the polyatomic reactant does not significantly affect the rotational inhibition factors. We explain the rotational inhibition by considering the fact that the

DOI: 10.1021/acs.jpca.5b06212
J. Phys. Chem. A 2015, 119, 12231−12237

tumbling rotation counteracts the orientation effects caused by ion-dipole interactions. This orientation effect is stronger in the $F^- + CH_3Cl$ reaction, which may diminish the rotational effects. The spinning rotation can hinder the complex formation, thereby reducing the reactivity.

Recent studies showed that rotational excitations, especially the tumbling rotation, promote the Cl/O + CHD_3 reactions.[13−15] The present study shows opposite rotational effects for the $F^- + CH_3F/CH_3Cl$ S_N2 reactions. Our detailed QCT analysis provides some insight into the mechanistic origin of the *JK*-specific rotational effects; however, a clear picture has not emerged that explains all the subtle features of the collision energy dependence of the *JK*-specific rotational enhancement/inhibition factors. The present study may inspire future experimental and theoretical work to investigate the rotational mode specificity in S_N2 reactions. One may study the deuterium substitution effect, which slows the spinning rotation, and/or the *JK*-dependent reactivity of CH_3Y with different nucleophiles.

■ AUTHOR INFORMATION

Corresponding Author

*E-mail: czako@chem.elte.hu.

Present Address

†Department of Physical Chemistry and Materials Science, University of Szeged, Rerrich Béla tér 1, H-6720 Szeged, Hungary.

Notes

The authors declare no competing financial interest.

■ ACKNOWLEDGMENTS

G.C. thanks the Scientific Research Fund of Hungary (OTKA, PD-111900) and the János Bolyai Research Scholarship of the Hungarian Academy of Sciences for financial support. The computing facility provided by NIIF on the High Performance Computing supercomputer at the University of Szeged is acknowledged.

■ REFERENCES

(1) Sathyamurthy, N. Effect of Reagent Rotation on Elementary Bimolecular Exchange Reactions. *Chem. Rev.* **1983**, *83*, 601−618.

(2) Urban, J.; Tino, J.; Klimo, V. Quasi-classical Trajectory Study of the Effect of Reactant Rotation in H(D) + HBr → H_2(HD) + Br Reactions. *Chem. Papers* **1991**, *45*, 257−263.

(3) Jiang, B.; Li, J.; Guo, H. Effects of Reactant Rotational Excitation on Reactivity: Perspectives from the Sudden Limit. *J. Chem. Phys.* **2014**, *140*, 034112.

(4) Camden, J. P.; Bechtel, H. A.; Ankeny Brown, D. J.; Zare, R. N. Comparing Reactions of H and Cl with C−H Stretch-Excited CHD_3. *J. Chem. Phys.* **2006**, *124*, 034311.

(5) Yoon, S.; Holiday, R. J.; Crim, F. F. Control of Bimolecular Reactivity: Bond-Selected Reaction of Vibrationally Excited CH_3D with Cl($^2P_{3/2}$). *J. Chem. Phys.* **2003**, *119*, 4755−4761.

(6) Liu, K. Perspective: Vibrational-Induced Steric Effects in Bimolecular Reactions. *J. Chem. Phys.* **2015**, *142*, 080901.

(7) Li, J.; Jiang, B.; Song, H.; Ma, J.; Zhao, B.; Dawes, R.; Guo, H. From ab Initio Potential Energy Surfaces to State-Resolved Reactivities: X + H_2O ↔ HX + OH [X = F, Cl, and O(^{3}P)] Reactions. *J. Phys. Chem. A* **2015**, *119*, 4667−4687.

(8) Espinosa-García, J. Role of the C−H Stretch Mode Excitation in the Dynamics of the Cl + CHD_3 Reaction: A Quasi-classical Trajectory Calculation. *J. Phys. Chem. A* **2007**, *111*, 9654−9661.

(9) Czakó, G.; Bowman, J. M. Reaction Dynamics of Methane with F, O, Cl, and Br on ab Initio Potential Energy Surfaces. *J. Phys. Chem. A* **2014**, *118*, 2839−2864.

(10) Xu, Y.; Xiong, B.; Chang, Y.-C.; Ng, C. Y. Communication: Rovibrationally Selected Absolute Total Cross Sections for the Reaction $H_2O^+(X^2B_1;\ v_1^+v_2^+v_3^+ = 000;\ N^+_{Ka+Kc+})$ + D_2: Observation of the Rotational Enhancement Effect. *J. Chem. Phys.* **2012**, *137*, 241101.

(11) Li, A.; Li, Y.; Guo, H.; Lau, K.-C.; Xu, Y.; Xiong, B.; Chang, Y.-C.; Ng, C. Y. Communication: The Origin of Rotational Enhancement Effect for the Reaction of H_2O^+ + H_2 (D_2). *J. Chem. Phys.* **2014**, *140*, 011102.

(12) Zhang, Z.; Zhang, D. H. Effects of Reagent Rotational Excitation on the H + CHD_3 → H_2 + CD_3 Reaction: A Seven Dimensional Time-Dependent Wave Packet Study. *J. Chem. Phys.* **2014**, *141*, 144309.

(13) Liu, R.; Wang, F.; Jiang, B.; Czakó, G.; Yang, M.; Liu, K.; Guo, H. Rotational Mode Specificity in the Cl + CHD_3 → HCl + CD_3 Reaction. *J. Chem. Phys.* **2014**, *141*, 074310.

(14) Czakó, G. Quasiclassical Trajectory Study of the Rotational Mode Specificity in the O(^{3}P) + $CHD_3(v_1 = 0,1, JK)$ → OH + CD_3 Reactions. *J. Phys. Chem. A* **2014**, *118*, 11683−11687.

(15) Wang, F.; Pan, H.; Liu, K. Imaging the Effects of Reactant Rotations on the Dynamics of the Cl + $CHD_3(v_1 = 1, |J,K\rangle)$ Reaction. *J. Phys. Chem. A* **2015** DOI: 10.1021/acs.jpca.5b03524.

(16) Yan, P.; Meng, F.; Wang, Y.; Wang, D. Y. Energy Efficiency in Surmounting the Central Energy Barrier: a Quantum Dynamics Study of the OH + CH_3 → O + CH_4 Reaction. *Phys. Chem. Chem. Phys.* **2015**, *17*, 5187−5193.

(17) Yan, P.; Wang, Y.; Li, Y.; Wang, D. Y. A Seven-Degree-of-Freedom, Time-Dependent Quantum Dynamics Study on the Energy Efficiency in Surmounting the Central Energy Barrier of the OH + CH_3 → O + CH_4 Reaction. *J. Chem. Phys.* **2015**, *142*, 164303.

(18) Manikandan, P.; Zhang, J.; Hase, W. L. Chemical Dynamics Simulations of X^- + CH_3Y → XCH_3 + Y^- Gas-Phase S_N2 Nucleophilic Substitution Reactions. Nonstatistical Dynamics and Nontraditional Reaction Mechanisms. *J. Phys. Chem. A* **2012**, *116*, 3061−3080.

(19) Wester, R. Velocity Map Imaging of Ion−Molecule Reactions. *Phys. Chem. Chem. Phys.* **2014**, *16*, 396−405.

(20) Tachikawa, H. Direct Ab Initio Dynamics Study on a Gas Phase Microsolvated S_N2 Reaction of $F^-(H_2O)$ with CH_3Cl. *J. Phys. Chem. A* **2000**, *104*, 497−503.

(21) Szabó, I.; Császár, A. G.; Czakó, G. Dynamics of the F^- + CH_3Cl → Cl^- + CH_3F S_N2 Reaction on a Chemically Accurate Potential Energy Surface. *Chem. Sci.* **2013**, *4*, 4362−4370.

(22) Zhang, J.; Xu, Y.; Chen, J.; Wang, D. Y. A Multilayered-Representation, Quantum Mechanical/Molecular Mechanics Study of the CH_3Cl + F^- Reaction in Aqueous Solution: the Reaction Mechanism, Solvent Effects and Potential of Mean Force. *Phys. Chem. Chem. Phys.* **2014**, *16*, 7611−7617.

(23) Xie, J.; Otto, R.; Mikosch, J.; Zhang, J.; Wester, R.; Hase, W. L. Identification of Atomic-Level Mechanisms for Gas-Phase X^- + CH_3Y S_N2 Reactions by Combined Experiments and Simulations. *Acc. Chem. Res.* **2014**, *47*, 2960−2969.

(24) Szabó, I.; Telekes, H.; Czakó, G. Accurate ab Initio Potential Energy Surface, Thermochemistry, and Dynamics of the F^- + CH_3F S_N2 and Proton-Abstraction Reactions. *J. Chem. Phys.* **2015**, *142*, 244301.

(25) Szabó, I.; Czakó, G. Revealing a Double-Inversion Mechanism for the F^- + CH_3Cl S_N2 Reaction. *Nat. Commun.* **2015**, *6*, 5972.

(26) Hase, W. L. *Encyclopedia of Computational Chemistry;* Wiley: New York, 1998; pp 399−407.

DOI: 10.1021/acs.jpca.5b06212
J. Phys. Chem. A 2015, 119, 12231−12237